JOURNAL OF CATALYSIS 85, 224–236 (1984)

The Initiation and Growth of Filamentous Carbon from α-Iron in H_2, CH_4, H_2O, CO_2, and CO Gas Mixtures

ALBERT SACCO, JR., PRADEEP THACKER, TZYH NAN CHANG, AND ANTHONY T. S. CHIANG

Department of Chemical Engineering, Worcester Polytechnic Institute, Worcester, Massachusetts 01609

Received April 22, 1983; revised July 19, 1983

The initiation and growth mechanisms of filamentous carbon over iron foils were studied at 900 K and 1 bar pressure. Various gas mixtures of CO, CO_2, CH_4, H_2, and H_2O were used to fix the solid phase compositions based on nonequilibrium phase diagrams. Solid phase compositions were verified using X-ray and electron diffraction. Gravimetric analysis indicated that in dry gas mixtures the initial rate of fractional weight gain was a direct function of the $P_{CO}P_{H_2}$ product; for water containing experiments it was related to the $P_{H_2O}/P_{H_2}P_{CO}$ ratio. X-Ray diffraction analysis of the solid suggested that the maximum rate of fractional weight gain coincided with complete carbiding of the "surface" layers. Examination of the foils in an electron microscope indicated the surface breaks up into a nodular morphology, and these nodules are comprised of filamentous carbon. An initiation mechanism is proposed which assumes that Fe_3C acts to increase over all surface area through surface breakup and also acts as a catalyst for carbon deposition and subsequent filament growth.

INTRODUCTION

The formation of carbon on metals has been and continues to be of importance when carbon-bearing gases contact metals at high temperatures. Uncontrolled carbon deposition can result in corrosion of metals as well as the deactivation of metal catalysts. Although there are many forms of deposited carbon, one of the most interesting and potentially damaging is called filamentous carbon.

Carbon filaments or fibers form on many metals, notably nickel, iron, and cobalt. The fibers themselves are uniform in width (between 500 and 1000 Å) (*1*) and are generally cylindrical in shape, although flat ribbons and twisted filaments (*2*) have been reported. The cylindrical fibers appear to have a hollow central core. Metallic crystals are often found at the end of these filaments and in some cases metallic fragments are found throughout their length. These metal crystallites are believed to be catalytically active for carbon deposition and are called "growth" crystals. The fiber shaft has been reported by Oberlin *et al.* (*3*) to be "tree-like," consisting of an inner ring of well-ordered carbon adjacent to the hollow core, and an outer carbon layer which is less ordered but more dense. The filaments can have lengths over 1 μm and BET areas as high as 100 m^2/g. Fiber C/Fe ratios can be well in excess of 100. If hydrogen is available during formation, the C/H atomic ratios in the filaments can vary between 10 and 30; and they are generally found to increase with temperature (*4*).

The growth mechanism and to a lesser extent the initiation mechanism for filaments have been speculated on by many investigators: Ruston *et al.* (*5*); Baker *et al.* (*6*); Boehm (*2*); Oberlin *et al.* (*3*); and Rostrup-Nielsen and Trimm (*7*). However, no complete mechanism has been proposed which can explain the various, often conflicting, data.

Baker *et al.* (*8*) and Baker and Chludzinski (*9*) used controlled atmosphere electron microscopy to measure the activation energy associated with filament growth. Their data suggest that the controlling

0021-9517/84 $3.00
Copyright © 1984 by Academic Press, Inc.
All rights of reproduction in any form reserved.

mechanism for fiber growth is diffusion of deposited carbon through the growth crystallite. Also, a small amount of surface diffusion was postulated. Although the mechanism suggested by Baker and co-workers has been accepted by many investigators, it has not received universal acceptance. For example, Oberlin *et al.* (*3*) from a detailed study of the morphology of filaments formed from iron suggested a two-step mechanism. They hypothesized that the "tree-like" structure they observed was a result of an inner ring formed by the decomposition of a metal–metal hydrocarbon species which surface diffused from the front end of the crystal to the rear where it decomposed. The thicker less crystalline outer ring was then formed by a secondary pyrolysis process. This mechanism, also suggested by Baird *et al.* (*10*), seems qualitatively to fit nicely most of the observed fiber morphologies. In general, most of the other mechanisms suggested by investigators are to a greater or lesser extent combinations of these proposals.

Even if one accepts the central idea for a given growth mechanism, there seems to be much disagreement as to the details. As an example of this, Baker *et al.* (*6*) suggested that the mass flux necessary for his proposed growth mechanism is the result of a temperature gradient developed due to the exothermicity of the carbon deposition reactions. The data of Evans *et al.* (*11*), Robertson (*12*), and Keep *et al.* (*13*) seem to support this contention, while the findings of Rostrup-Nielsen and Trimm (*7*), Rostrup-Nielsen (*14*), and Bernardo and Lobo (*15*) suggest exothermicity is unnecessary.

Finally, and of critical importance, which solid phase(s) catalyze carbon deposition and subsequent fiber formation is unclear. Although this is a problem encountered for all metals which form filaments, we direct our discussion to some relevant studies that used iron. Ruston *et al.* (*5*) reported the formation of iron carbide (Fe_3C) within the bulk of an iron foil which was found to support fiber growth. However, they identified the fiber growth crystal as Fe_7C_3 by using X-ray diffraction. Renshaw *et al.* (*16*) and Ratliff (*17*) contended that their X-ray diffraction data is open to other interpretation. They suggest that the data of Ruston *et al.* (*5*) could be interpreted as oxide formation. In the study by Oberlin *et al.* (*3*) selective area electron diffraction was used to identify the growth crystal. They reported that d-spacings for cementite (Fe_3C) and α-Fe were the only ones present in the growth crystals in their work. Finally, from the works of Baker *et al.* (*6*) and Baker and Chludzinski (*9*), the reported activation energy suggests that carbon diffuses through the reduced metal (e.g., iron), and thus implies that the reduced metal is the growth crystal.

The approach we used in our laboratory was to carefully control and characterize solid phase composition in order to determine the effect of various solid phases on carbon formation and filament growth. It was hoped that based on his information, an initiation mechanism could be proposed to help in the understanding of carbon filament formation.

EXPERIMENTAL

Complete details on the experimental procedure and apparatus (Fig. 1) are given by Sacco and Caulmare (*18*) and only a brief description will be presented here.

All experiments were performed with 6 × 6 × 0.25-mm polycrystalline iron foils (>99.99% pure). The reactor assembly was supported on a vibration frame, which allowed continuous monitoring of the foil's weight change (operational sensitivity 10^{-6} g) using a Cahn 2000 electrobalance. The reactor was operated isothermally with a West SCR stepless proportional temperature controller. Reaction temperature was 900 ± 1°K and the pressure was 1 bar. Carbon was deposited or oxidized from multicomponent gas mixtures consisting of H_2, H_2O, CH_4, CO, and CO_2. The gas feed rate was 20 cm^3/s (STP). This value was chosen to avoid any mass transfer limitations,

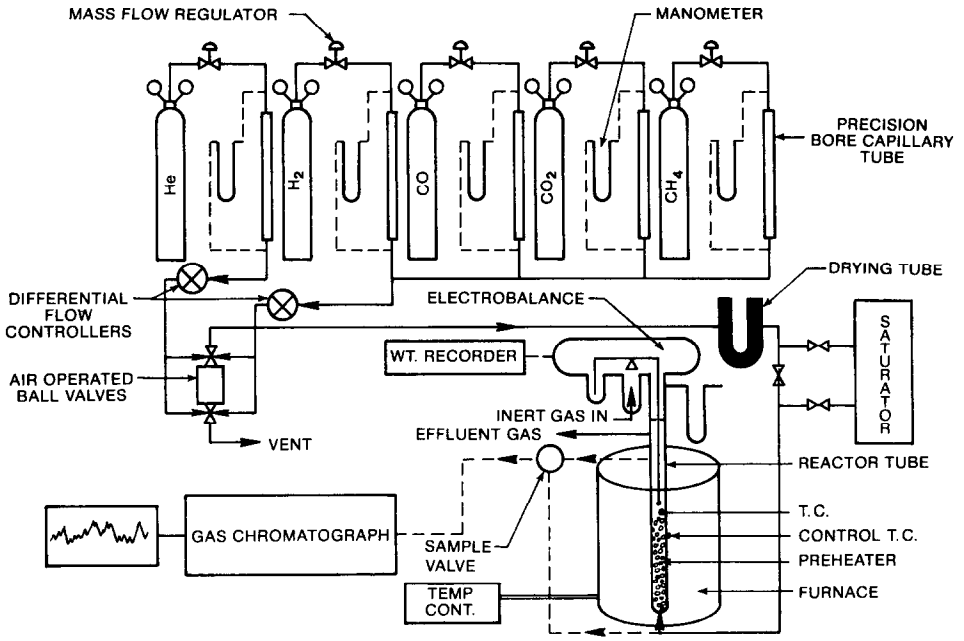

FIG. 1. Experimental apparatus.

based on the rate of carbon deposition from CO. Inlet and effluent gas compositions were taken periodically (usually every 10–20 min) using an on-line Sigma 1 gas chromatograph. At the conclusion of an experiment, the reaction gases were vented to the atmosphere and the system cooled down in helium or in some cases the sample was directly quenched in a liquid nitrogen bath. All samples were examined using optical and electron microscopy.

METHODOLOGY

To ascertain which solid iron phases are catalytic for carbon deposition and from these to determine which are involved in fiber growth, phase diagrams are helpful. The usefulness of these diagrams for this system has been demonstrated by Sacco and Reid (*19*). Figure 2 is a phase diagram showing the Fe_3C/Fe–gas (dashed curve), Fe_xO/Fe–gas (curve concave down), and the C_β–gas[1] equilibria at 900 K and 1 bar pressure. These equilibria phase boundaries divide the triangular surface into various phase fields. Thus, for a gas mixture represented by position M, the solid iron phase thermodynamically favored is Fe_3C (cementite). In this region carbon would also be expected to form if Fe_3C catalyzes carbon deposition. Similarly, for a mixture represented by position X, carbon should be oxidized if Fe_xO (wustite) is a catalyst for carbon oxidation.

These diagrams allow one to precondition the surface (e.g., carbide) and then feed a multicomponent gas mixture that favors only the preconditioned surface. In this way the surface phase(s) can be controlled *in situ*. Alternately, if the oxidizing, reducing, or carbiding reactions are faster than the carbon deposition reaction(s), one

[1] It is recognized that the form of carbon associated with filaments is, although highly crystalline, not graphitic (*20*). Thus, the boundary for the carbon–gas equilibrium will be somewhat shifted from that shown. The only works dealing with this were over nickel (*14, 21*) and therefore are not appropriate here. However, at the temperature of this work (900 K) using these data, the shift is not great, the maximum shift moving the C_β–gas equilibrium only very slightly upward.

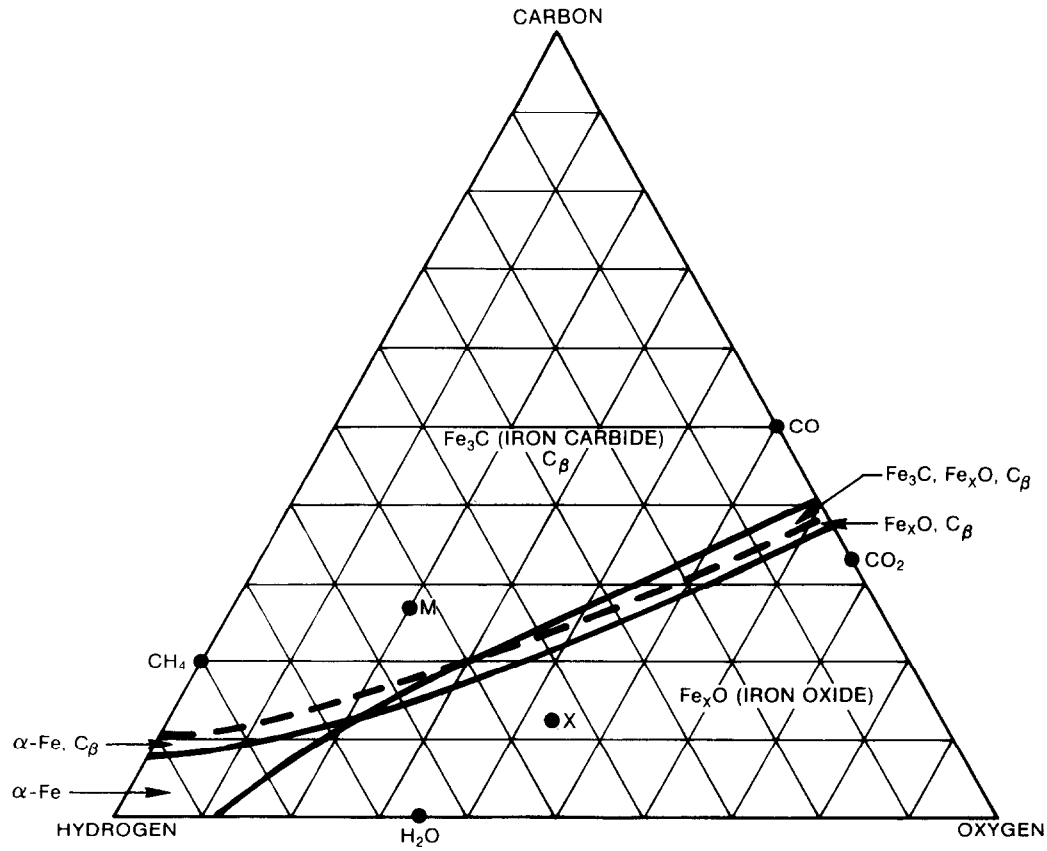

FIG. 2. Phase diagram for the α-Fe, Fe_xO, Fe_3C, C_β, and gas system.

can change from one phase field to another and observe the effect on carbon deposition of the new surface phase.

SOLID PHASE IDENTIFICATION

Two techniques were used to identify solid phase compositions: X-ray diffraction and electron diffraction. X-Ray diffraction patterns were obtained directly from the iron foil after cleaning off any loose carbonaceous deposits. These data were obtained using a Philips XRG-3000 X-ray generator with Ni-filtered Cu$K\alpha$ radiation. The electron diffraction data were determined with a JEOL-100C STEM. The samples prepared for the electron diffraction studies were obtained by extracting thin iron films from fused quartz wafers on which they had been exposed to the reaction gases. The results obtained by both these techniques were consistent with each other. For brevity as well as ease of presentation, only the X-ray data will be presented. Figure 3 shows the kind of spectra found.

Spectrum (a) is for an unreacted iron foil. The spectrum at degrees 2θ of 44.7°, 65°, 82.3° represents α-iron (ferrite). The small peak at degrees 2θ of approximately 32° best matches that of iron carbonate. Spectra (b) and (c) represent one experiment performed in the carbide phase field for 7 min and one performed in the α-iron region for 30 min, respectively. In both of these cases, to obtain a close approximation to the actual solid composition, the iron foils were quenched with liquid nitrogen directly from reaction conditions.

Spectrum (b) indicates that during reaction the intensity of the α-iron spectrum de-

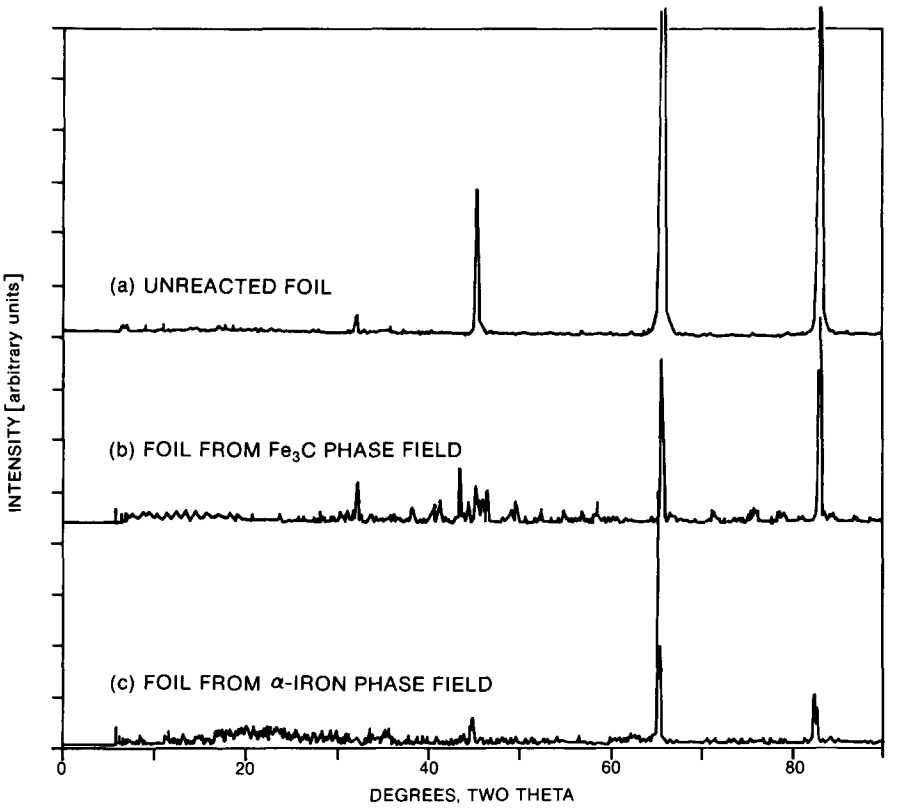

FIG. 3. X-Ray diffraction data (Phillips XRG-3000, Cu$K\alpha$).

creases, while the spectrum characteristic of Fe_3C begins to appear (at approximately 45°, 2θ). All the proper d-spacings were present leaving no doubt as to its identification. The longer the foil was exposed to the reaction gases, the greater the intensity of the Fe_3C spectrum and conversely the lower the intensity of the ferrite spectrum. This spectrum was typical of all experiments made in the carbide region. Likewise, spectrum (c) is typical of the spectrum obtained anywhere in the ferrite region. These data along with the electron diffraction data confirm that for the conditions used in this work a phase diagram based on bulk thermodynamic data is adequate for fixing solid composition. The doublets observed in spectra (b) and (c) are the result of both the stress introduced by the precipitation of cementite in the ferrite and that caused by the quenching procedure.

RESULTS AND DISCUSSION

The majority of experiments were performed by heating iron foil up to 900 K in pure hydrogen (Airco, Grade 4.5). The desired gas phase composition was then fed to the reactor. A representative set of experiments is presented in Table 1. Their locations on the phase diagram are shown in Figure 4. As illustrated by Fig. 4, with the exception of the experiment indicated with the open square, carbon deposition only occurred in the region where cementite (Fe_3C) was thermodynamically favored to form (dark symbols). Examination of the surface disclosed only a small amount of free carbon; the vast majority of the carbon was observed to be in the filamentous form. The experiment represented by the open square is close to the Fe_3C/α-Fe phase boundary. With the uncertainty of the thermodynamic

TABLE 1

Composition of Typical Experiments

Symbol	Mole percent					Comments
	H_2	CO	CH_4	CO_2	H_2O	
▲	42.1	30.9	25.0	2.0	0.00	Wt. gain
⬢	66.2	2.8	30.8	0.20	0.00	Wt. gain
●	60.0	10.7	26.9	2.40	0.00	Wt. gain
■	54.7	15.3	21.7	5.3	3.0	Wt. gain
▼	45.0	27.0	13.4	6.4	8.2	Wt. gain
♦	42.4	27.8	14.0	15.8	0.0	Wt. gain
□	65.2	2.70	30.4	0.20	1.50	No wt. gain
▽	62.1	7.8	16.3	2.6	11.2	No wt. gain
○	76.0	0.50	8.50	15.0	0.0	No wt. gain
△	39.0	22.0	7.6	17.8	13.6	No wt. gain

data for Fe_3C this could be in either phase field. The fact that no carbon was observed, suggests, consistent with the other results, that it is in the α-Fe phase region. Figure 5 illustrates typical surface features. Micrograph (A) shows the iron foil prior to reaction. As shown, the foil's surface is relatively smooth with some scratches and pits. After reaction, micrograph (B), the surface appears to breakup into a nodular morphology. This type of structure has been reported by Sacco and Reid (*23*) under similar conditions on a steel wool surface. Higher magnification micrographs (C,D) indicate that these nodules are composed of carbon filaments. These fibers all had electron dense tips and a hollow central core (Fig. 6).

A. Weight Gain Measurements

Figure 7 is a plot of the initial weight gain in micrograms versus reaction time in min-

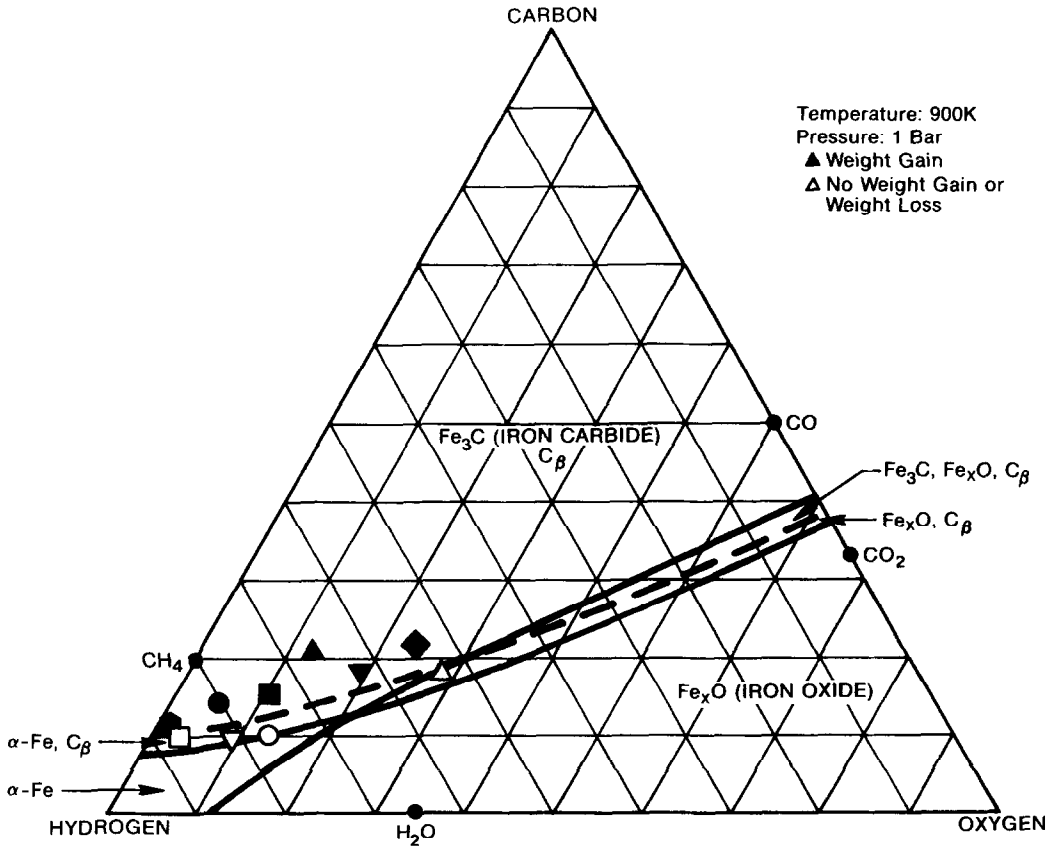

FIG. 4. Evidence that suggests cementite is necessary for the initiation and growth of filamentous carbon over iron.

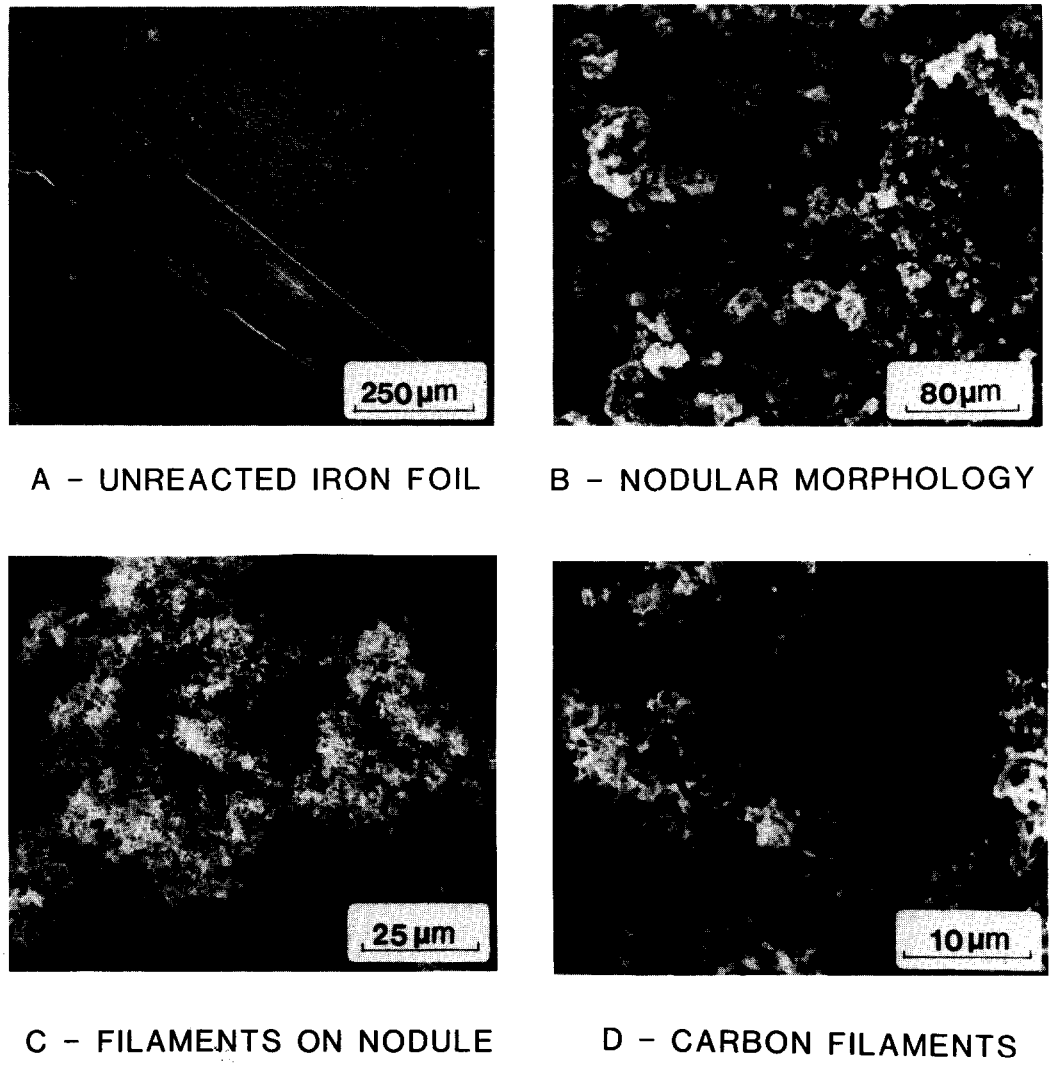

FIG. 5. Typical surface features.

utes. These data are from the six carbon depositing experiments indicated in Table 1. Generally it was found that the larger the product of the carbon monoxide and hydrogen partial pressure the greater the weight gain. This relationship is consistent with the rate expression proposed by Manning (*24*) for the reaction of carbon monoxide and hydrogen over iron. However, if water was present this general observation did not always hold (e.g., inverted triangles).

If these data are replotted as rate of fractional weight gain (i.e., normalize the change in weight to the initial weight–area) versus time a qualitatively clearer picture emerges. These data, Fig. 8, show that the most rapid increase in fractional weight gain occurs initially. At a later time the rates are observed to level off or drop slightly followed by a period of constant rate of weight gain. All experiments performed in the carbide region resulted in this kind of behavior. For the water-free experiments, the higher initial rates were found to be associated with higher values of the product ($P_{CO}P_{H_2}$). This suggests that either

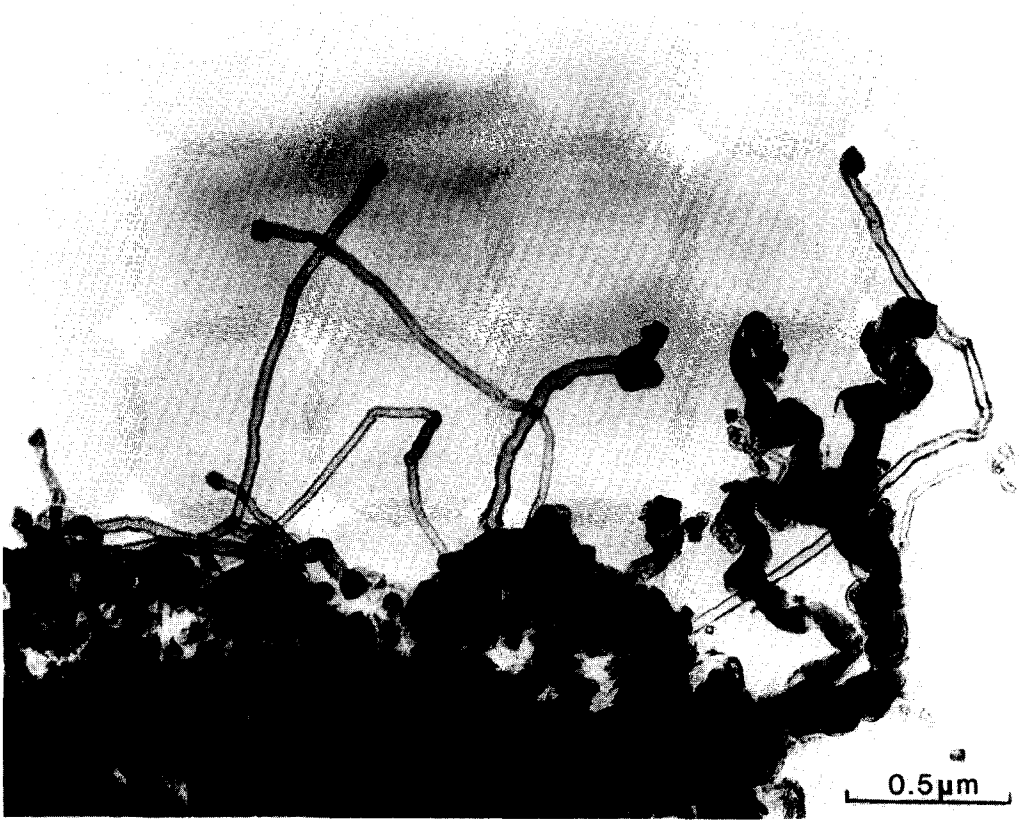

FIG. 6. Filamentous carbon.

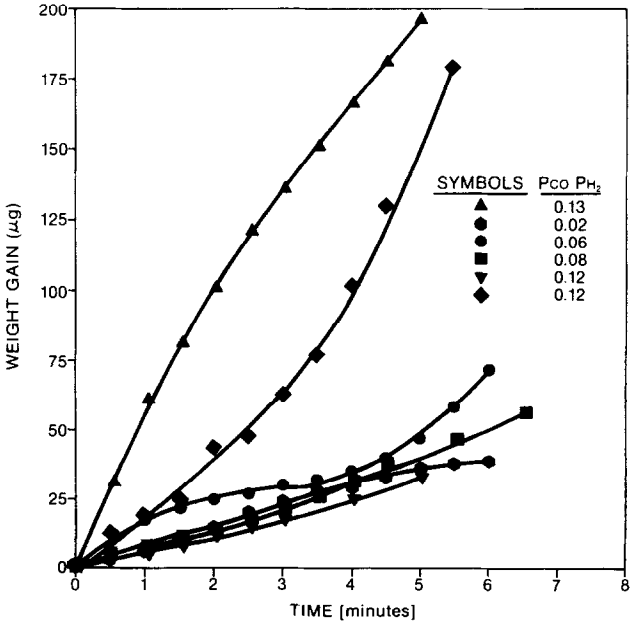

FIG. 7. Initial weight gain versus time in the carbide region for various H_2, CO, CO_2, CH_4, and H_2O at 900 K and 1 bar.

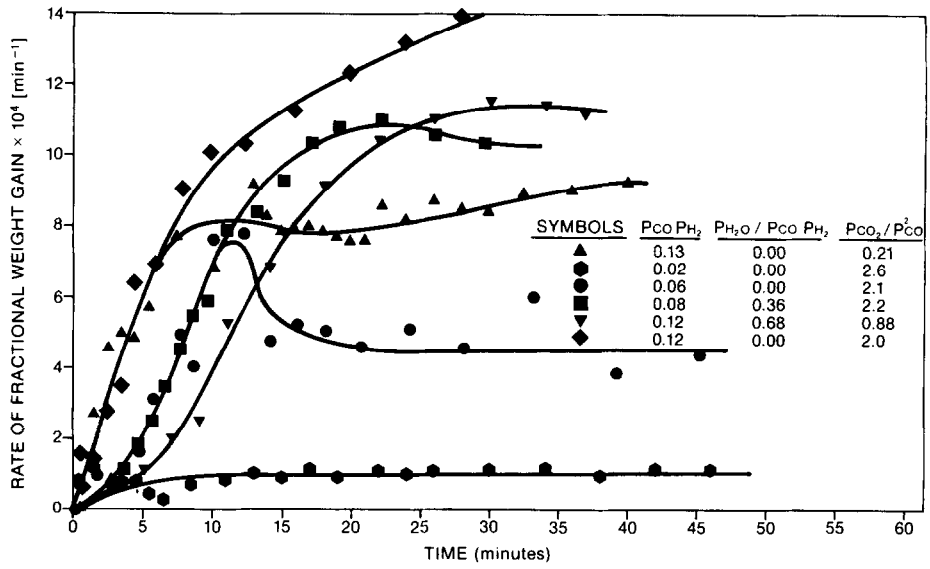

FIG. 8. Rate of weight gain versus time for various H_2, CO, CO_2, CH_4, and H_2O mixtures in the carbide region at 900 K and 1 bar.

carbon deposition is primarily the result of Reaction 1:

$$H_2 + CO \rightleftharpoons H_2O + C_\beta \qquad K = 2.46 \quad [1]$$

or that carbides formed by Reaction 2 catalyze or in some other way enhance carbon deposition from reactions such as Reactions 1, 3, and 4:

$$H_2 + CO + 3Fe \rightleftharpoons Fe_3C + H_2O \qquad K = 1.49 \quad [2]$$

$$CH_4 \rightleftharpoons 2H_2 + C_\beta \qquad K = 3.11 \quad [3]$$

$$2CO \rightleftharpoons CO_2 + C_\beta \qquad K = 5.69 \quad [4]$$

Although it is tempting to try to develop and test a kinetic mechanism based on these results, this is difficult since the active catalytic area is constantly changing with time as filaments initiate, develop, and grow.

A further complication is added when the experiments containing water are examined. For reaction mixtures with water the criterion of a higher ($P_{CO}P_{H_2}$) resulting in a faster initial rate of weight gain seems untrue (e.g., the position of the inverted triangles and squares in Fig. 8). Since water is present in these experiments, the reverse reactions for Reactions 1 and 2 could be expected to occur. This would affect the observed rate of weight gain or fractional weight gain. Assuming both these reverse reactions are catalyzed, this effect can be qualitatively determined by examining the $P_{H_2O}/P_{CO}P_{H_2}$ ratio. The closer this ratio is to the value of the equilibrium constant the smaller is the chemical potential driving force for reaction, and theoretically the slower the reaction. Thus, if both Reactions 1 and 2 are catalyzed in the forward and reverse direction, one would predict that the experiment represented by the squares should have a faster initial rate than the experiment indicated by the inverted triangles. This is what is observed, and it seems to qualitatively explain the relative position of water containing experiments to each other for all such experiments performed in the carbide phase field. The ratios for the Boudouard reaction (P_{CO_2}/P_{CO}^2) are also shown in Fig. 8. No qualitative behavior could be predicted from these. In addition, it appeared that the amount of methane

present had no effect on the rates of fractional weight gain for the conditions run.

B. Carbide Formation

A series of experiments was performed to determine if the formation of Fe_3C in the bulk could be related to the observed rate of weight gain curves. Experiments were made under the conditions indicated by the dark triangles in Table 1 and Fig. 8. Periodically during these experiments the iron foils were quenched directly from reaction conditions with liquid nitrogen. Since there were only two major phases present, the total intensities for each phase could be used to indicate the relative amount of each phase in the sample. Fig. 9 shows the data obtained. As time on stream increases, the amount of cementite formed increases and the amount of α-iron present decreases. The major decrease in the intensity of the α-iron signal and the increase in the cementite signal occurs over the first 8–12 min. This coincides nicely with the period of increased rate of fractional weight gain shown for the dark triangles in Fig. 8. Also, the rate of fractional weight gain shown for the dark triangles levels off at, or close to, its maximum rate. This leveling off is close to the same period where the carbide intensity reaches a maximum and the α-iron signal decreases to a minimum. This behavior suggests the cementite formation enhances carbon deposition by increasing the relative surface area through surface breakup caused by precipitation of the carbide in the iron matrix. The fact, however, that weight gain (carbon deposition) does not occur in the α-iron region though carbon deposition is thermodynamically favored supports the contention that carbide(s) are necessary catalytically, at least initially, for carbon deposition to occur. Whether or not the carbon deposited is catalytic is unclear at this time. Our observation of the surface after reaction suggests that the region of constant rate of weight gain reflects a fixed number of growing carbon filaments.

To help clarify the effect of cementite formation, a foil was precarbided using pro-

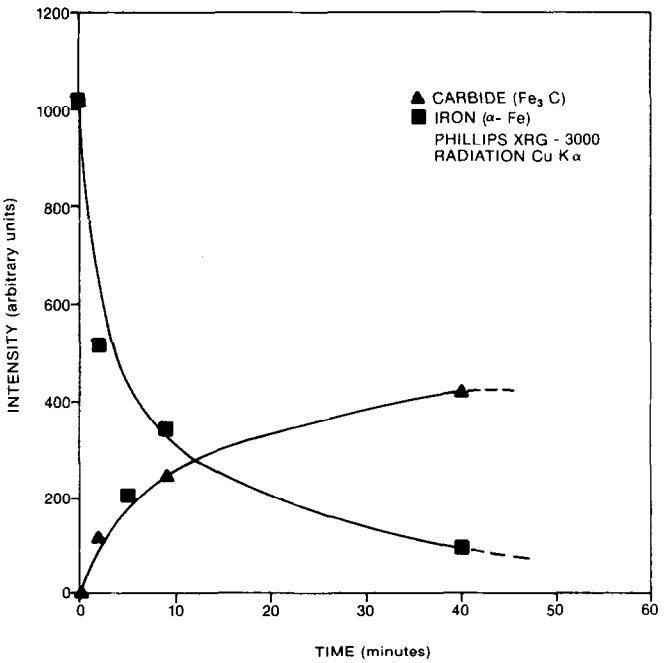

FIG. 9. X-Ray diffraction data of iron foils reacting at 900 K with CO, CO_2, H_2, and CH_4 and quenched in liquid N_2.

pane at 563 K. Browning *et al.* (*25*) and Podgurski *et al.* (*26*) have shown that carbiding in propane at 563 K resulted in Fe_2C formation with no evidence of carbon formation. This Hägg carbide was reported to transform to Fe_3C at 673 to 723 K. Podgurski *et al.* (*26*) observed this Fe_3C to decompose to Fe and C in a few hours if heated to 773 K in a vacuum. However, we did not see any evidence of Fe_3C decomposition as the iron foil was rapidly (5–10 min) heated from 563 K to 900 K in propane. At 900 K a gas composition thermodynamically favoring Fe_3C formation, as indicated by dark triangles in Table 1, was introduced. The results are plotted in Fig. 10. As indicated, the initial rate of fractional weight gain for the precarbided sample was 3 to 4 times greater than that of the unconditioned foil. Eventually both rates come together.

The interpretation of this data is not obvious. The data suggest that there are initially more sites available for carbon deposition and subsequent filament growth. We hypothesize that on these sites carbon is rapidly deposited to form both "free carbon" and filamentous carbon. "Free carbon" is used here to mean any carbon not associated with filamentous growth. Baker *et al.* (*8*) showed that filament growth is a diffusion controlled process; thus, if the deposition of carbon is initially faster on certain sites than its diffusion, some of the active sites or filament growth will be blocked thereby eventually reducing the overall rate of carbon deposition. Therefore, the "free carbon" blocks that portion of the surface from further reaction. However, those fibers formed extend out from the surface, are not covered by "free carbon," and continue to grow. The data imply that in both cases the number of filaments initially formed are equal.

The fact that an iron surface must be carbonized prior to substantial carbon deposition occurring has been reported by Tsao (*27*). Tsao ran pure carbon monoxide over reduced iron disks at 903 K. He used Mössbauer spectroscopy to analyze his samples.

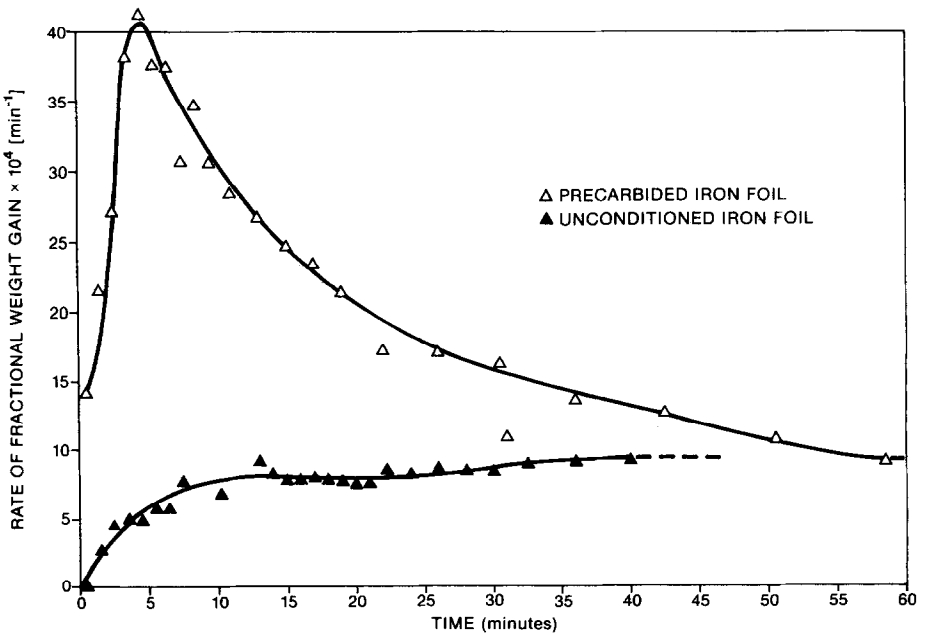

FIG. 10. Comparison between a precarbided and unconditioned iron foil at 900 K and 1 bar under identical gas phase composition.

He found free carbon only formed after the surface was almost completely carbided. These results support our own. However, Baker *et al.* (*28*) in a recent paper, reported that particles of Fe_3C supported on graphite and exposed to 2 Torr acetylene were not catalytic for the growth of filamentous carbon. This apparent discrepancy with the results reported here may be explained if the following assumptions are made. It may be assumed that either Fe_3C does not catalytically decompose acetylene as it appears to decompose CO or it may be necessary to have a two-phase metal interface present (e.g., Fe_3C/α-Fe) to provide the necessary solubility difference for carbon diffusion and subsequent filament growth. At this time either explanation is speculative and the role Fe_3C plays for different gas systems must still be evaluated.

CONCLUSIONS

These data suggest that cementite formation enhances, at least initially, the formation of carbon filaments from α-iron. The fact that carbon deposition and concomitant filament growth only occurs in the cementite phase field implies that cementite is a better catalyst for carbon deposition than is α-iron. However, the observation (Fig. 5) that the surface breaks up into nodules gives rise to another possibility. Perhaps, when cementite is thermodynamically favored, the surface breaks up due to cementite precipitation. This may result in a substantial increase in surface area relative to the reduced foil. This in turn is observed as an increased rate of carbon deposition. If one accepts this hypothesis, the fact that virtually no weight gain is observed in the α-iron phase field implies α-iron is not a particularly good catalyst for filament growth, and it requires a large effective area. In fact, the contribution of cementite is probably twofold: one, it catalyzes carbon deposition; and two, it breaks up the surface which creates a large increase in surface area.

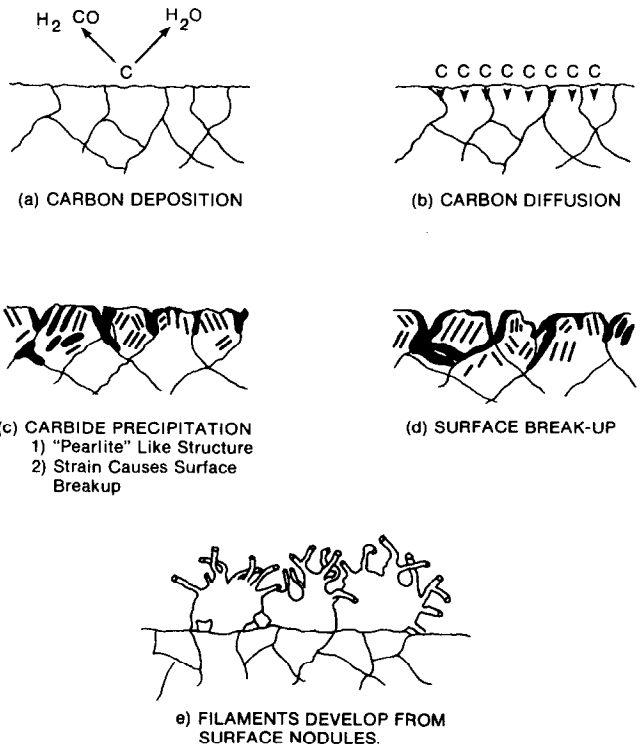

FIG. 11. Proposed initiation mechanism for the development of filamentous carbon on α-iron.

Using these results as a basis, the following initiation mechanism is hypothesized (Fig. 11). Initially (a) carbon is deposited from carbon monoxide and hydrogen mixtures. This carbon (b) then diffuses into the surface and (c) cementite begins to precipitate at energetically favorable areas such as grain boundaries, edges, and matrix dislocations (at this stage when the surface is chemically etched, nital solution, a "pearlite-like" structure is observed). The process continues and in so doing introduces stress into the foil surface. The surface then breaks up (d) forming a rough nodule like morphology. Filaments grow from these nodules (c). The controlling mechanism for filament growth is assumed, in agreement with Baker *et al.* (*6*), to be the diffusion of carbon through the reduced metal. Our calculations suggest this mass flux is established as the result of the solubility difference between carbon at the α-iron/Fe_3C interface and that between α-iron and carbon itself.

ACKNOWLEDGMENT

The authors gratefully acknowledge the support and encouragement of the National Science Foundation through Grant CEP-7918173.

REFERENCES

1. MacIver, D. S., and Emmett, P. H., *J. Phys. Chem.* **59,** 1109 (1955).
2. Boehm, H. P., *Carbon* **11,** (1973).
3. Oberlin, A., Endo, M., and Kayama, T., *J. Crystal Growth* **32,** 335 (1976).
4. Walker, P. L., Jr., Rakszawski, J. F., and Imperial, G. R., *J. Phys. Chem.* Part I, **73,** 133 (1959); Part II, **73,** 140 (1959).
5. Ruston, W. R., Warzee, M., Hennaut, J., and Waty, J., *Carbon* **7,** 47 (1969).
6. Baker, R. T. K., Barber, M. A., Harris, P. S., Feates, F. S., and Waite, R. J., *J. Catal.* **26,** 51 (1972).
7. Rostrup-Nielsen, J., and Trimm, D. L., *J. Catal.* **48,** 155 (1977).
8. Baker, R. T. K., Harris, P. S., Thomas, R. B., and Waite, R. J., *J. Catal.* **30,** 86 (1973).
9. Baker, R. T. K., and Chludzinski, J. J., Jr., *J. Catal.* **64,** 464 (1980).
10. Baird, T., Fryer, J. R., and Grant, B., *Carbon* **12,** 591 (1974).
11. Evans, E. L., Thomas, J. M., Thrower, P. A., and Walker, P. L., *Carbon* **11,** 441 (1973).
12. Robertson, S. D., *Carbon* **8,** 365 (1970).
13. Keep, W. C., Baker, R. T. K., and France, J. A., *J. Catal.* **47,** 232 (1977).
14. Rostrup-Nielsen, J. R., *J. Catal.* **27,** 343 (1972).
15. Bernardo, C. A., and Lobo, L. S., *in* "Catalyst Deactivation," Proceedings, International Symposium, Antwerp (B. Delmon and G. F. Froment, Eds.), Vol. 6, p. 409. Elsevier Scientific, New York, 1980.
16. Renshaw, G. D., Roscoe, C., and Walker, P. L., Jr., *J. Catal.* **18,** 164 (1970).
17. Ratliff, J. T., Ph.D., Georgia Institute of Technology, 1968.
18. Sacco, A., Jr., and Caulmare, J. C., "Coke Formation on Metal Surfaces." ASC Symposium Series, 70,202, 1982.
19. Sacco, A., Jr., and Reid, R. C., *AIChE J.* **25,** 839 (1979).
20. McCarty, J. G., and Wise, H., *J. Catal.* **57,** 406 (1979).
21. Manning, M. P., Garmirian, J. E., and Reid, R. C., *Ind. Eng. Chem. Process Des. Dev.* **21,** 404 (1982).
22. Caulmare, J. C., M. S., Worcester Polytechnic Institute, 1981.
23. Sacco, A., Jr., and Reid, R. C., *Carbon* **17,** 459 (1979).
24. Manning, M. P., Sc.D., Massachusetts Institute of Technology, 1976.
25. Browning, L. C., DeWitt, T. W., and Emmett, P. H., *J. Amer. Chem. Soc.* **72,** 4211 (1950).
26. Podgurski, H. H., Kummer, J. T., DeWitt, T. W., and Emmett, P. H., *J. Amer. Chem. Soc.* **72,** 5382 (1950).
27. Tsao, T., Ph.D., Carnegie-Mellon University, 1974.
28. Baker, R. T. K., Alonzo, J. R., Dumesic, J. A., and Yates, D. J. C., *J. Catal.* **77,** 74 (1982).